
XVI INTERNATIONAL CONGRESS OF THE MEXICAN HYDROGEN SOCIETY

MEMORY 2016

GENERAL INDEX

GENERAL INDEX

GENERAL INDEX

GENERAL INDEX

GENERAL INDEX

GENERAL INDEX

Hydrogen production improved mixed oxide TiO_2-ZrO_2 photocatalyst as semiconductor

Alejandro Pérez-Larios[1,2*], Ricardo Gomez[2].

[1]Universidad de Guadalajara, Centro Universitario de los Altos, Depto. Ciencias Biologicas, Carretera a Yahualica km. 7.5, Tepatitlán de Morelos, Jalisco, México. 47600.
[2]Universidad Autónoma Metropolitana-Iztapalapa, Depto. de Química, Área de Catálisis, Grupo ECOCATAL, Av. San Rafael Atlixco No 189, D.F., México 09340.

(*) alarios@cualtos.udg.mx

Abstract

In this study the synthesis of the semiconductor oxide TiO_2 doped with ZrO_2 varying concentrations was using for hydrogen production. The photocatalysts were characterized by N2 phisisortion studies, scanning electron microscopic-energy dispersive analysis, X-ray diffraction studies, UV-vis and Raman spectroscopy. The anatase phase in these materials showed high superficial area, the studies of UV-Vis absorption showed a diminish in the energy band gap in function of the zirconium content. The Raman spectrum indicates that crystalline structure of TiO_2 was modified for the presence of cerium. In the photocatalytic activity, the materials showed an increase in the hydrogen production, where, the maximum hydrogen production was achieved at 10 wt. % of the zirconium content.
keywords: Hydrogen; photocatalysts; semiconductor; TiO_2; Mixed oxide

I. INTRODUCTION (*HEADING 1*)

Hydrogen is an attractive alternative sustainable clean energy carrier because of the depletion of fossil fuel reserves and the environmental pollution caused by continuous burning of fossil [1,3]. Hydrogen is currently obtained from nonrenewable natural gas, naphta, heavy oil, methanol, biomass, wastes, coal, petroleum and water, but could be generated from renewable resources such as biomass [4,8]. Water decomposition by means of sunlight mimics photosynthesis by converting water into H_2 and O_2 using inorganic photo-semiconductors that catalyze the water-splitting reaction [9,10]:

$$H_2O \rightarrow \frac{1}{2}O_2 + H_2 \quad (g)$$

Water decomposition using sunlight on semiconductor photocatalysts has attracted intense research interest since the pioneering work on a photo-electrochemical cell conducted [11]. This work has stimulated the research for the overall water splitting reaction using particulate photocatalysts that was first realized in 1980 [12] who reported stoichiometric evolution of hydrogen and oxygen. Since these ground-breaking works, many papers have been published on the impact of different semiconductor materials on photocatalytic water splitting performance [13-14]. These studies clearly prove that the energy conversion efficiency of water splitting is principally determined by the properties of the semiconductors used as photocatalysts. Light-driven water splitting is initiated when a photo-semiconductor absorbs light photons with energies greater than its band gap energy (Eg). This absorption creates excited photoelectrons in the conduction band (CB) and holes in the valence band (VB) of the semiconductor. After that, the second step in photochemical water splitting consists of charge separation and the migration of photogenerated electron–hole pairs from the bulk of the semiconductor towards the reaction sites on the photocatalysts surface. The final step of the photocatalytic process involves the surface chemical reactions. The photo-generated electrons (e^-) and holes (h^+) that migrate to the surface of the photocatalysts without recombination can reduce and oxidize, respectively, water molecules adsorbed onto the surface of the semiconductor to produce gaseous oxygen and hydrogen by the following reactions:

Oxidation: $H_2O + 2h^+ \rightarrow 2H^+ + \frac{1}{2}O_2$

Reduction: $2H^+ + 2e^- \rightarrow H_2$

Overall reaction: $H_2O \rightarrow \frac{1}{2}O_2 + H_2$

This phenomenon explains the slow hydrogen production by photocatalytic water splitting using TiO_2 alone [15,16]. Some oxide in combine with TiO_2 in the formation of mixed oxide is also known to increase photocatalytic performance via inhibiting the recombination of electrons and holes for the evolution of H_2 [17].

It was recently suggested by Verykios and co-workers, that decomposition of organics and H_2-production can be used in tandem [18, 19]. The idea is that H_2-production efficiency is increased by using an electron-donor contaminant (sacrificial reagent), which will ultimately result in enhancement of the H_2 production rate with simultaneous degradation of the organic substrate'' [18]. In the majority of the studies published in the literature, methanol was used as sacrificial reagent [19–23], further examples include the decomposition

of various azo-dyes [18], glucose [24], glycerol [25] and formic acid [26], etc.

In the present study we have prepared mixed oxide TiO_2-ZrO_2 photocatalysts using sol-gel method and tested their efficiency for hydrogen generation. Thus, the principal objective of the work is to develop TiO_2-ZrO_2 mixed oxide photocatalysts for hydrogen production from aqueous solution ethanol-water under irradiation with UV-visible light. Characterization of the catalysts was done following standard procedures.

II. Experimental

2.1 Synthesis and Characterization of Materials

The mixed oxide TiO_2-ZrO_2 nanostructures were prepared by the sol-gel method using titanium butoxide (IV) (Aldrich 97%) and their respective salt as precursor: 44 mL of 1-butanol (Aldrich 99.4 %) and 18 mL of distilled wáter containing the appropriate average $C_{20}H_{28}O_8Zr$ (Strem Chemicals 99%), In the preparation of each of the series of obtaining materils with 1.0, 3.0, 5.0 y 10.0 wt %, were mixed and added few drops of HNO_3 to obtain a pH=3 in the solution. 44 mL were prepared butoxide titanium (IV) to add the above solution at 70°C under reflux (with a molar ratio of 8) this solution was mixed under magnetic stirring to form the gel. The gel was dried at 100 °C for 24h and the solid was ground to a fine powder in an agate mortar. The xerogel obtained was calcined at 500° C for 5 h in an air atmosphere with a heating rate of 1°C/min; finally the product was ground again. As a reference the sample of pure TiO_2 was prepared in the same manner described but not added salt as precursors.

2.2 Materials Characterization

2.2.1 Thermal Analysis (TGA)

Thermograms for thermogravimetric analysis (TGA) were determined on a Perkin Elmer Analyse, modelo Diamond TG/DTA instrument. It was operated un der static atmosphere of air, covering the range from room temperature to 800º C with a heating rate of 10 ºC/min. Samples of about 50 mg of dry gel were analized [27].

2.2.2 Energy dispersive X-ray spectroscopy (EDS)

Energy dispersive X-ray spectroscopy, EDS best known, is an analytical technique used for the elemental analysis or chemical characterization of a simple. Analysis were carried out in a JEOL JSM-6390LV Scanning Electron Microscope instrument.

2.2.3 Nitrogen adsorption

Nitrogen adsorption-desorption isotherms were obtained with an automatic Quantachrome Autosorb 3B instrument. Prior to the nitrogen adsorption, all the samples were outgassed overnight at 200° C. The specific surface areas of the samples were calculated from the nitrogen adsorption-desorption isotherms using the BET method, and the mean pore size diameter from the desorption isotherms using the BJH method.

2.2.4 X-ray diffraction

The obtained TiO_2 and TiO_2-ZrO_2 powders were analyzed by X-ray diffraction using a Bruker D-8 Advance apparatus. The diffraction intensity as a function of the diffraction angle (2θ) was measured between 4 and 70°, using a step of 0.03° and a counting time of 0.3 s per step [30,31].

2.2.5 RAMAN Spectroscopy

Raman spectra ewre obtained using a renishaw spectrometer model Invia MicroRaman using 100x objective and as radiation source an argón laser monochromatic with wavelength 514.5 nm wmission corresponding to green light and a power of 25 mW. In the analysis equipment were placed 10 mg of powdered sample of solids. The Raman shift range for analysis was of 0 a 1200 cm^{-1}[30,32].

3.2.6 UV-Visible Spectroscopy by reflactance difusse.

The UV–Vis absorption spectra were obtained with a Cary 100 UV–Vis spectrophotometer (VARIAN) coupled with an integration sphere for diffuse reflectance studies. A sample of MgO with 100% of reflectance was used as a reference. The diffuse reflectance spectrum was obtained and transformed to a magnitude proportional to the extinction coefficient (α) through the Kubelka-Munk function, equation (a):

$$F(R) = \frac{(1-R)^2}{2R} \qquad \text{(a)}$$

Eg value was calculated from the plot of Kubelka-Munk function F(R) vs wavelength of the absorbed light.

2.2.7 Hydrogen production

The schematic reactor system is described in a previous report. The photo-activity for the hydrogen generation was evaluated using a homemade Pyrex reactor of 250 mL containing 200 mL of water-ethanol solution (1:1 vol/vol) and 0.1 g of catalysts. The irradiation was made using a high pressure Hg pen-lamp (with a radiation of 254 nm and intensity of 2.2 mW/cm^2) encapsulated in a quartz tube immersed in the water solution. The amount of hydrogen produced was followed by using a gas chromatograph (VARIAN CP-3800) equipped with a thermal conductivity detector and with a 5A column molecular sieve (30m length, 0.35mm ID and 50 mm OD).

3. Result and discussion

3.1 Thermogravimetric analysis (TGA-DTA)

The principal analysis of thermogravimetric (TGA) of the samples of TiO_2-ZrO_2 (1.0, 3.0, 5.0 and 10.0 wt %) it can show in the figures 2 and 3.

The Fig. 2 and 3shown the lost weight (Tg) and the curves of analysis differential thermal (DTA) of the mixed oxide TiO_2-ZrO_2 without thermal treatment. For the sample with 1 % de Zr in the figure 2 shown the curves of TG at 1 % wt of Zr, where it show a peak endothermic a low temperatures of 80° C, with a lost weight of 1.0 %, that go associates to lost residual water and trapped solvent in the particles. of 80° C to 250° C, 250° C to 270° C, 270° C to 350° C and 350° C to

460° C, it has tree peaks exothermic corresponding to 8.9 %, 10.5 % and 18.42 % of lost weight respectively, that could be atribuirse to the combustion of organic residual strong retained, same that it evidence of calcination of gel. After of 460° C it has a sintering of material that suggest a crystallization to anatase phase [27].

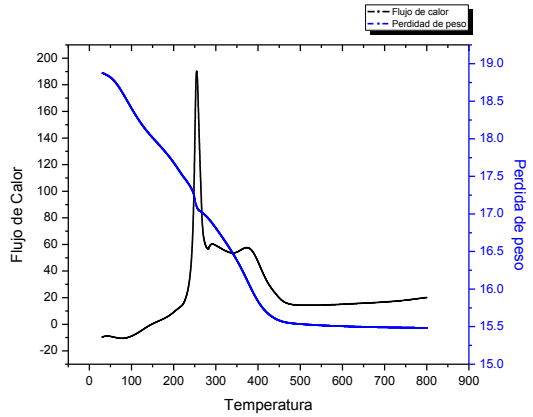

Figure 2. TGA-DTA of mixed oxide of TiO_2-ZrO_2 at 1 %.

Figure 3 show the lost weigth (TG) and the curves of the analysis differential thermal (DTA) of mixed oxide TiO_2-ZrO_2 at 5 % wt. of Zr, without thermal treatment. The curves of TG show the lost endothermic weight to small temperature of 50° C to 100° C it has a peak, with lost weight of 4.76 %, that ranging associated to residual water and trapped solvent in the particles. Of 100° C to 220° C, 220° C to 400° C, it has two exothermic peaks corresponding to 9.0 % and 19.04 % of lost weight respectively that go associated at organic material. After of the 450° C it has a winterization of material that suggest more stability of anatase phase [27].

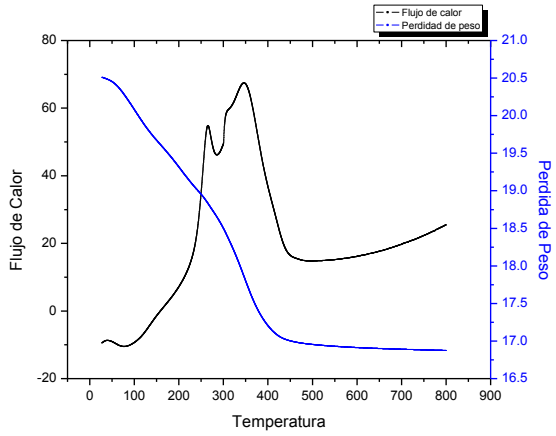

Figura 3. TGA-DTA of mixed oxide TiO_2-ZrO_2 at 10 %.

3.2 Energy Dispersive Spectroscopy (EDS)

Spectra EDS were obtained, which are shown in table 1, it can be seen the presence of ZrO_2, these results can be observed the presence of Zr^{4+}, which is not identifiable by X-ray technique, will be appreciated that the material surface has unevennes, you can also be seen in the micrographs some agglomerates granular appearance. The presence of particles with large unevenness is likely due to the fact that the formation of mixed oxide, in this cases TiO_2-ZrO_2, are in the Surface of TiO_2.

Tabla 1. Elemental Analysis EDS of mixed oxide TiO_2-ZrO_2

Percent	Ti	Zr
1	98.68	1.32
3	96.72	3.28
5	93.42	6.42
10	91.68	8.32

3.3 N_2 Physisorption

The data of the specific áreas of the samples which were calcined at 500° C are reported in table 2. The results show that the specific área by the BET method when the % Zr increases, increased respect to reference of TiO_2 (64 m^2/g). the profiles of the isotherms and the distribution of pore size respectively, we suggest that are type 4 [2], this adsorption isotherm perfectly corresponds to that determined by Hackley and Anderson [3], with hysteresis type 2 (IUPAC), accordingto the classification of de boer [4] which are in solid matrices with uniform pores having capillary condensation and have mesoporous structure and is attributed to the monolayer adsorption data distribution pore size are reported in table 2 (1.0, 3.0, 5.0 and 10.0 % wt of Zr) although wide is unimodal with maximum (4 nm) located in the mesoporous region [5].

Tabla 2. Textural properties, Band gap (Eg) of mixed oxide of TiO_2-ZrO_2.

ZrO_2	Área	Pore diameter	Eg	Cell Parameters		Cristalite size
(% Wt)	(m^2/g)	(nm)	(eV)	a (nm)	c (nm)	D (nm)
1.0	91	5.6	3.05	0.56	0.948	7.8
3.0	147	7.7	3.14	0.58	0.956	7.9
5.0	157	7.8	3.20	0.66	0.950	8.7
10.0	138	6.5	3.15	0.78	0.156	9.9
TiO_2	64	6.5	3.20	0.377	0.943	5.7

3.4 X-ray Difracction (XRD)

Figure 4 XRD patterns of the samples of TiO_2 and mixed oxide TiO_2-ZrO_2. XRD patterns show the anatase phase (JCPDD: 21-1272) formed in the TiO_2. Peaks appear in 2Θ=25.4°, 38°, 48°, 54°, 63°, corresponding to the diffraction patterns of (101), (112), (200), (211) and (204) respectively of anatase phase. It has been reported that ZrO_2 peaks does not appear in the present study in 2Θ: 30°, 35°, 50° y 60°, corresponding to the diffraction patterns of (101), (002), (112) and (211). The tetragonal phase of ZrO_2 not appear in the present study [6]. Vishwanathan et al. Has been reported that 10 % by weight does not contribute to any change in morphology in the mixed oxide, as well as high crystallinity in the existing particles [7]. These results suggest that some of Zr^{4+} cations were incorporated within the network of titania, as evidence increase in cell parameter with respect to Zr (Table 2). However, high specific area shown in the mixed oxide is highly likely that the ZrO_2 was sufficiently dispersed to form clusters on the Surface of titania and not detectable by

XRD [8] these data are supported with RAMAN and EDS spectroscopy.

The cristal size, D, of the samples was estimated from half with (β) of the peak 2θ = 25.4° by the Scherrer formula:

$$D = \frac{K\lambda}{\beta \cos\theta}$$

The values are reported in table 2, the cristal size is in the range of nanometers (7.8 to 9.9 nm) which was obtained in all samples.

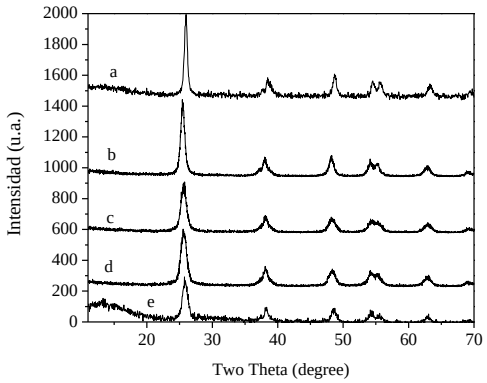

Figure 4. X-Ray diffractograms for mixed oxide TiO_2-ZrO_2

3.5 RAMAN Spepctroscopy

Figure 5 shows the RAMAN spectra of the samples TiO_2-ZrO_2, with concentrations of Zr^{2+} (1.0, 3.0, 5.0 and 10.0 %). Al peaks are characteristic signs of the anatase phase which has a shift in wavelength of 145 cm^{-1}, 395 cm^{-1}, 513 cm^{-1} and 640 cm^{-1} [9], these peaks correspond to the 5 modes of absorption of this active phase Raman of which overlapped two of the located at 519 cm^{-1} [10], which suggest that the ZrO_2 be embedded in the network of the titania. On the other hand these peaks decrease as the content of Zr^{2+} is increased, indicating a significant decrease in the cristalilinity of the mixed oxide. These result are consistent with XRD, not corresponding to the rutile phase (240 cm^{-1}, 442 cm^{-1} and 606 cm^{-1}) [11] or broquita (450 cm^{-1}, 365cm^{-1}, 320 cm^{-1} and 245 cm^{-1}) [12], where smalls crystal size correspond to smaples with high content of Zr.

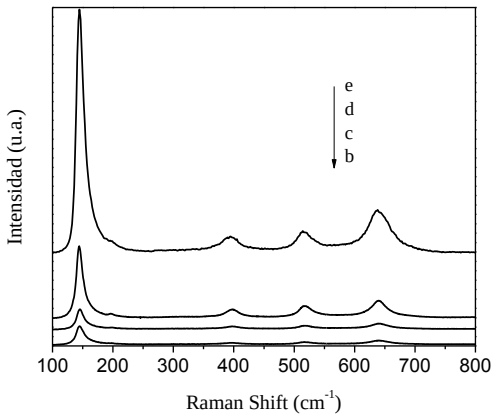

Figura 5. Raman spectra of the simple TiO_2-ZrO_2

3.6 UV-Vis spectroscopy

As to UV-visible spectrum of the sol-gel TiO2 calcined at 500° C (Fig. 6) is observed (at ~ 356 nm) corresponding to electronic transitions of Ti-O-Ti bonds in octahedral coordination absorption. It has been reported [13] that the anatase phase is characterized by an absorption starting near 450 nm with an inflexion near 370 nm accompanied by a plateau between 330 and 230 nm. This signal originates from the charge transfer transition → O2- Ti^{4+} corresponding to the excitation of electrons from the valence band (O2p with character) to the conduction band (with Ti 3d character) [14]. The position of this band with an energy gap of 3.2 eV characterizes in the TiO2 anatase phase as a semiconductor.

The UV-Vis studies were conducted in order to investigate the effect of ZrO_2 in the photophysical properties of TiO_2-ZrO_2 semiconductors. All samples a shift between these wavelengths, which can be attributed to the transitions of the Ti-O electrons TiO_2 nanocrystals TiO_2-ZrO_2 and the results show small bands in the red region (3.05-3.2 eV) for TiO_2-ZrO_2 samples of 1% to 10% by weight of Zr, compared to TiO_2 in anatase phase reference (3.2 eV) (Fig. 6) .

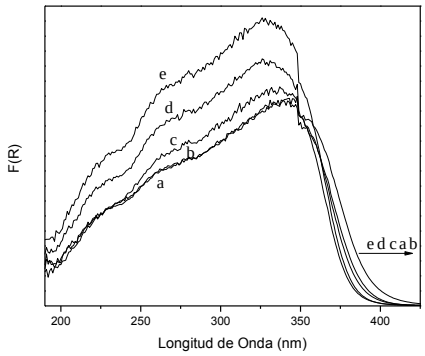

Figure 6. UV-Vis spectra by diffuse reflactance, samples TiO_2-ZrO_2

3.7 Hydrogen Production

In Figure 9, the hydrogen production is shown as a function of irradiation time for samples of TiO_2 and TiO_2-ZrO_2. It can be seen that the formation of hydrogen increases with respect to the weight percent of Zr^{4+}. Hydrogen production for titanium dioxide was 190 mol / h. an important effect of ZrO_2, regarding the content is observed. Forming TiO_2-ZrO_2 to 1% and TiO_2-ZrO_2 to 3% was 387 and 910 μmol/h, respectively, an increase of approximately 100% and for each of the catalysts 500%. H_2 production for TiO_2-ZrO_2 5% was 1600 μmol/h, while the maximum formation was obtained for TiO2-ZrO_2 catalyst 10% to 1,990 μmol/h, Fig. 7 The ZrO2 disappears as the reaction proceeds in the samples d and e (graph 7). These results are very interesting compared when used Au/TiO_2 [16] Pt-TiO_2 [17,18] Ag/TiO_2. [19].

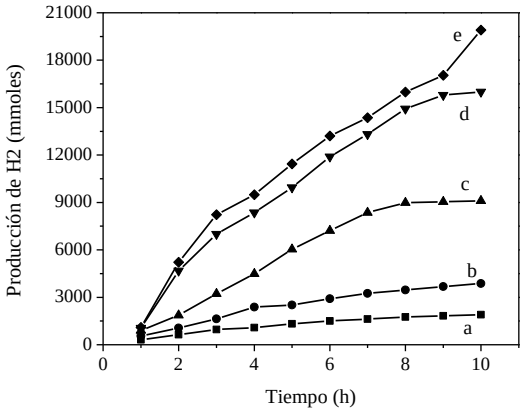

Figure 7. Profile of hydrogen production of mixed oxide TiO_2-ZrO_2

4. Conclusion

This study clearly demonstrates the advantages of the formation of mixed oxides such as ZrO_2-TiO_2, for photocatalytic hydrogen generation. Most TiO_2 parameters such as particle size, surface area, the anatase phase, OH groups on the surface and the thermal stability can be controlled in the formation of the mixed oxides by sol-gel method.

Although high ZrO_2 content of the specific area increases and crystallite sizes suffer the same effect. The photocatalytic activity was good from 5% ZrO_2, this is due to the number of transfers electrons to TiO_2 at ZrO_2. Chemical interactions of Zr-O-Ti in the mixed oxide is a major factor by which a high photocatalytic activity was taken into H_2 production. The study of UV-vis by diffuse reflectance can give strong evidence of changes in the transition states, and there are changes on the surface of oxides, so we suggest that there is a change of CB ZrO_2 of the CB surface of TiO_2 and facilitate the exchange of electrons between them. And preventing recombination of electrons and holes to increase the photocatalytic efficiency of TiO_2. Electron generation proves to be the most important in the photocatalytic activity of the mixed oxides as evidenced by UV-vis analysis after reaction factor.

REFERENCIAS

[1] Gratzel M. Photoelectrochemical cells.Nature 2001;414:338-44.

[2] Rostrup-Nielsen JR. Conversion of hydrocarbons and alcohols for fuel cells. Phys Chem Chem Phys 2001;3:283-8.

[3] Service RF. Hydrogen economy? Let sunlight do the work. Science 2007;315:789.

[4] Cortright RD, Davda RR, Dumesic JA. Hydrogen from catalytic reforming of biomass-derived hydrocarbons in liquid water. Nature 2002;418:964-7.

[5] Woodward J, Orr M, Cordray K, Greenbaum E. Biotechnology: enzymatic production of biohydrogen. Nature 2000;405: 1014-5.

[6] Bard AJ, Fox MA. Artificial photosynthesis: solar splitting of water to hydrogen and oxygen. Acc Chem Res 1995;28:141-5.

[7] Fujishima A, Honda K. Electrochemical photolysis of water at a semiconductor electrode. Nature 1972;238:37-8.

[8] Khan SUM, Al-shahry M, Ingler Jr WB. Efficient photochemical water splitting by a chemically modified n-TiO_2. Science 2002;279:2243-5.

[9] Maeda K, Teramura K, Lu D, Takata T, Saito N, Inoue Y, et al. Photocatalyst releasing hydrogen from water. Nature 2006; 440:295.

[10] Ishikawa A, Takata T, Kondo JN, Hara M, Kobayashi H, Domen K. Oxysulfide $Sm_2Ti_2S_2O_5$ as a stable photocatalyst for water oxidation and reduction under visible light irradiation (λ= 650 nm). J Am Chem Soc 2002;124:13547-53.

[11] Ashokkumar M. An overview on semiconductor particulate systems for photoproduction of hydrogen. Int J Hydrogen Energy 1998;23:427-38.

[12] Meissner D, Memming R, Kastening B. Photoelectrochemistry of cadmium sulfide. 1. Reanalysis of photocorrosion and flatband potential. J Phys Chem 1988;92:3476-83.

[13] J. Jitputti, Y. Suzuki, S. Yoshikawa. Synthesis of TiO_2 nanowires and their photocatalytic activity for hydrogen evolution.

[14] L.S. Yoong, E.K. Chong, B.K. Dutta. Development of copper doped TiO2 photocatalyst for hydrogen production under visible light. Energy 34 (2008) 1652-1661.

[15] Ha SP, Dong HK, Sun JK, Kyung SL. The photocatalytic activity of 2.5 wt.% Cu doped TiO_2 nano powder synthesized by mechanical alloying. J Alloy Compounds 2005;415:51–5.

[16] Ni M, Micheal KH, Dennis YCL, Leung KS. A review and recent development in photocatalytic water-splitting using TiO2 for hydrogen production. Renew Sust Energ Rev 2007;11:401–25.

[17] K. Maeda, H. Terashima, K. Kase, K. Domen. Nanoparticulate precursor route to fine particles of TaON and ZrO2-TaON solid solution and their photocatalytic activity for hydrogen evolution. App. Catal. A: Gral. 357 (2009) 206-212.

[18] Patsoura A, Kondraides DI, Verykios XE Appl Catal B 64 (2006) 171.

[19] Patsoura A, Kondraides DI, Verykios XE Catal Today 124 (2007) 94.

[20] Sreethawong T, Suzuki Y, Yoshikawa S C R Chimie 9 (2006) 307.

[21] Dubey N, Rayalu SS, Labhsetwar NK, Devotta S Int J Hydrogen Energy 33 (2008) 5958.

[22] Yin S, Sato T. J Photochem Photobiol A 169 (2005) 89.

[23] Khan MA, Akhtar MS, Woo SI, Yang O-B. Catal Commun 10 (2008) 1.

[24] Fu X, Long J, Wang X, Leung DYC, Ding Z, Wu L, Zhang Z, Li Z, Fu X. Int J Hydrogen Energy 33 (2008) 6484.

[25] Daskalaki VM, Kondarides DI (in press) Catal Today. 144 (2009) 75-80.

[26] Chen T, Wu G, Feng Z, Hu G, Su W, Ying P, Li C. Chin J Catal 29 (2008) 105.

[27] Xu Q., Anderson M. A., *J. Am. Ceram. Soc*. **77** (1994) 1939

[28] Brunauer S., Deming L. S., Deming W. E., Teller E., *J. Am. Chem. Soc*. **62** (1940) 1723.

[29] Hackley V. A., Anderson M. A., Spooner S., *J. Mater. Res*. **7** (1992) 2555
[30] de Boer J. H., van den Heuvel A., Linsen B. G., *J. Catal*. **3** (1964) 268
[31] Bosch G. P., Domínguez J. M., Zénith J., Rouffignac E., Guzmán O.,Tejeda J., "Técnicas Experimentales en la Caracterización de Catalizadores", Series Científicas IMP, México (1986).
[32] Dzwigaj S., Louis C., Breysse M., Cattenot M., Bellière V., Geantet C., Vrinat M., Blanchard P., Payen E., Inoue S., Kudo H., Yoshimura Y., *Appl. Catal.* B **41** (2003) 181.